



Guerin, G., Rugar, P. A., Molev, G., Manners, I., Hiroshi, J., & Winnik, M. (2016). Lateral Growth of 1D Core-Crystalline Micelles upon Annealing in Solution. *Macromolecules*, 49(18), 7001-7014.  
<https://doi.org/10.1021/acs.macromol.6b01487>

Peer reviewed version

License (if available):  
CC BY-NC

Link to published version (if available):  
[10.1021/acs.macromol.6b01487](https://doi.org/10.1021/acs.macromol.6b01487)

[Link to publication record in Explore Bristol Research](#)  
PDF-document

This is the author accepted manuscript (AAM). The final published version (version of record) is available online via ACS at <http://pubs.acs.org/doi/suppl/10.1021/acs.macromol.6b01487>. Please refer to any applicable terms of use of the publisher.

## University of Bristol - Explore Bristol Research

### General rights

This document is made available in accordance with publisher policies. Please cite only the published version using the reference above. Full terms of use are available:  
<http://www.bristol.ac.uk/red/research-policy/pure/user-guides/ebr-terms/>

**SUPPORTING INFORMATION****Lateral growth of 1D core-crystalline micelles upon annealing in solution**

Gerald Guerin,<sup>1</sup> Paul Rugar,<sup>2,3</sup> Gregory Molev,<sup>1</sup> Ian Manners,<sup>2</sup> Hiroshi Jinnai<sup>\*4</sup>, and Mitchell A. Winnik<sup>\*1</sup>

1. *Department of Chemistry, University of Toronto, 80 St. George Street, Toronto, ON, M5S 1H6*
2. *School of Chemistry, University of Bristol, Bristol UK, BS8 1TS*
3. *Current Address: Department of Chemistry, University of Alabama, Tuscaloosa, AL 35487, USA*
4. *Institute of Multidisciplinary Research for Advanced Materials, Tohoku University, Katahira, Aoba-ku, Sendai, 980-8577, Japan*

## SUPPORTING TABLES

**Table S1:** Summary of the static light scattering analysis of the seed fragments annealed at 50 °C and 75 °C using three different approaches: Zimm plot, Guinier plot and from the data fitting using the form factor of a rigid cylinder

Annealing temperature	$M_{wapp}$ (g/mol)		$R_g$ (nm)	
	50 °C	75 °C	50 °C	75 °C
Zimm plot	$1.4 \times 10^7$	$1.7 \times 10^7$	39	31
Guinier plot	$1.4 \times 10^7$	$1.7 \times 10^7$	37	29
Form factor <sup>a</sup>	$1.4 \times 10^7$	$1.7 \times 10^7$	38	29

a. Equations 2,3, main text

**Table S2:** Summary of the electron tomography image analysis performed on 11 seed fragments for the samples annealed at 50 °C and 75 °C

Annealing Temperature		length (nm)	width (nm)	height (nm)
50 °C	Ave (nm)	81	19	6
	$\sigma$ (nm)	59	2.4	0.6
75 °C	Ave (nm)	72	25	5
	$\sigma$ (nm)	30	5.8	0.9

a.  $\sigma$  is the standard deviation

## SUPPORTING FIGURES

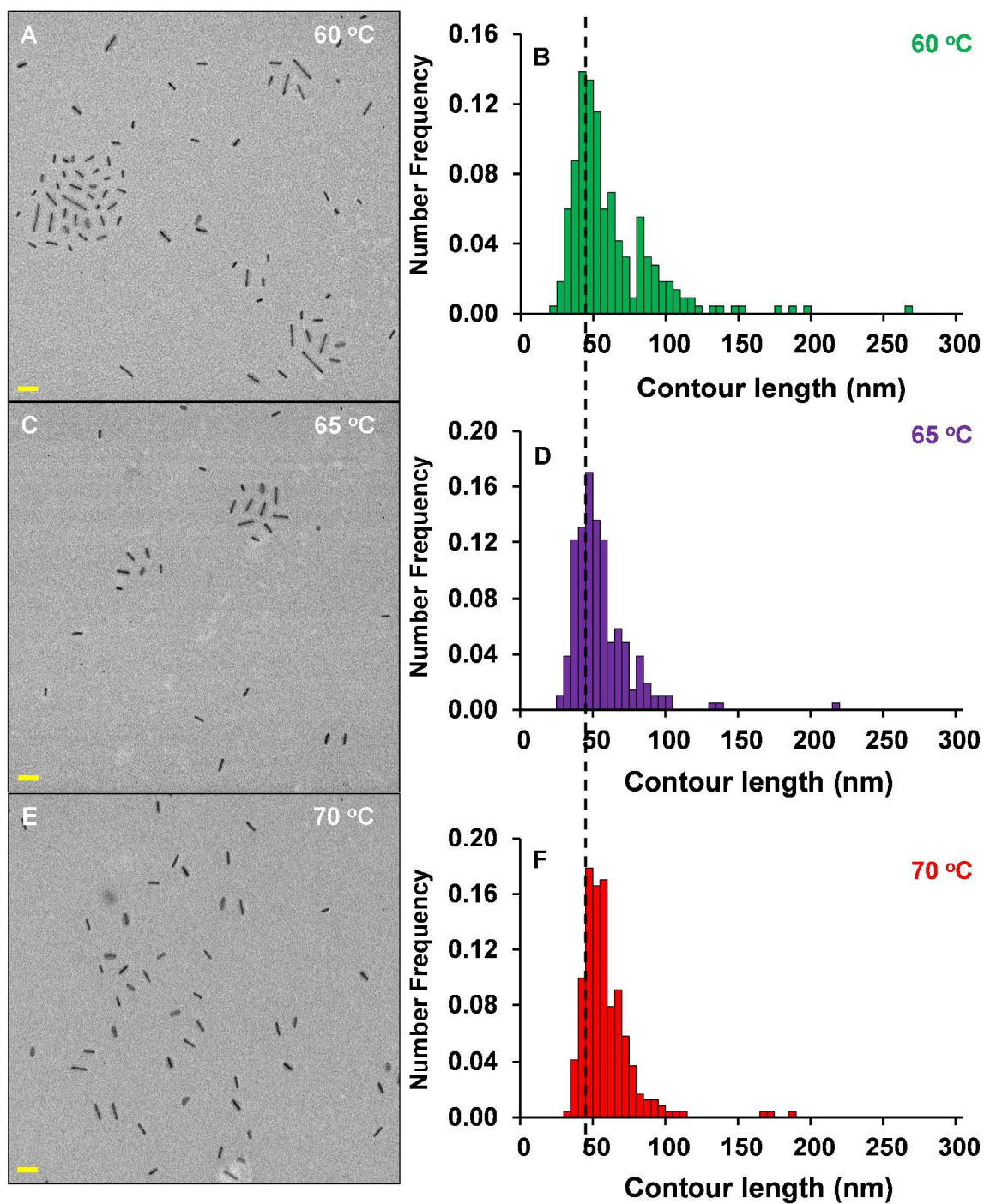


**Figure S1:** TEM images of PFS<sub>53</sub>-*b*-PI<sub>637</sub> seeds that were annealed at A) 60 °C, C) 65 °C, and E) 70 °C, and corresponding histograms of the length distribution of PFS<sub>53</sub>-*b*-PI<sub>637</sub> seeds that were annealed at B) 60 °C, D) 65 °C, and F) 70 °C., as evaluated from the TEM image analysis of more than 200 seeds for each sample. For all TEM images the scale bar corresponds to 100 nm.

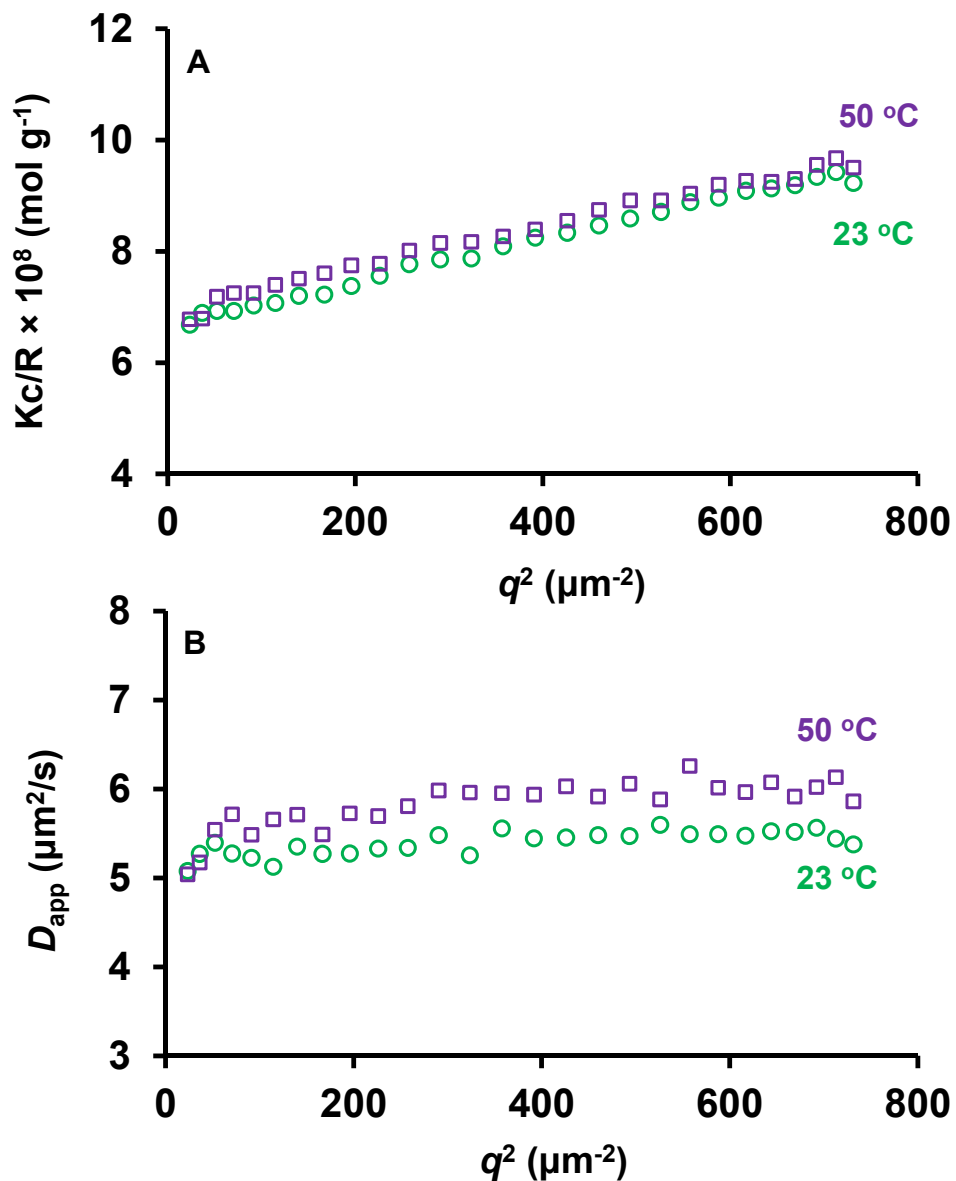


**Figure S2:** A) Plot of  $Kc/R$  versus  $q^2$  for a  $\text{PFS}_{53}\text{-}b\text{-PI}_{637}$  seed solution after sonication (green circles, denoted 23 °C) and annealed at 50 °C for 30 min (purple open squares). B) Plot of the diffusion coefficient,  $D_{\text{app}} = \Gamma/q^2$ , versus  $q^2$ , where  $\Gamma$  is the decay rate for the same solutions as in A). The concentration of the solution for the self-seeding experiments was  $c = 6.0 \text{ mg mL}^{-1}$  and the samples were diluted to a concentration  $c = 0.01 \text{ mg mL}^{-1}$  before performing the SLS and DLS experiments at 23 °C.

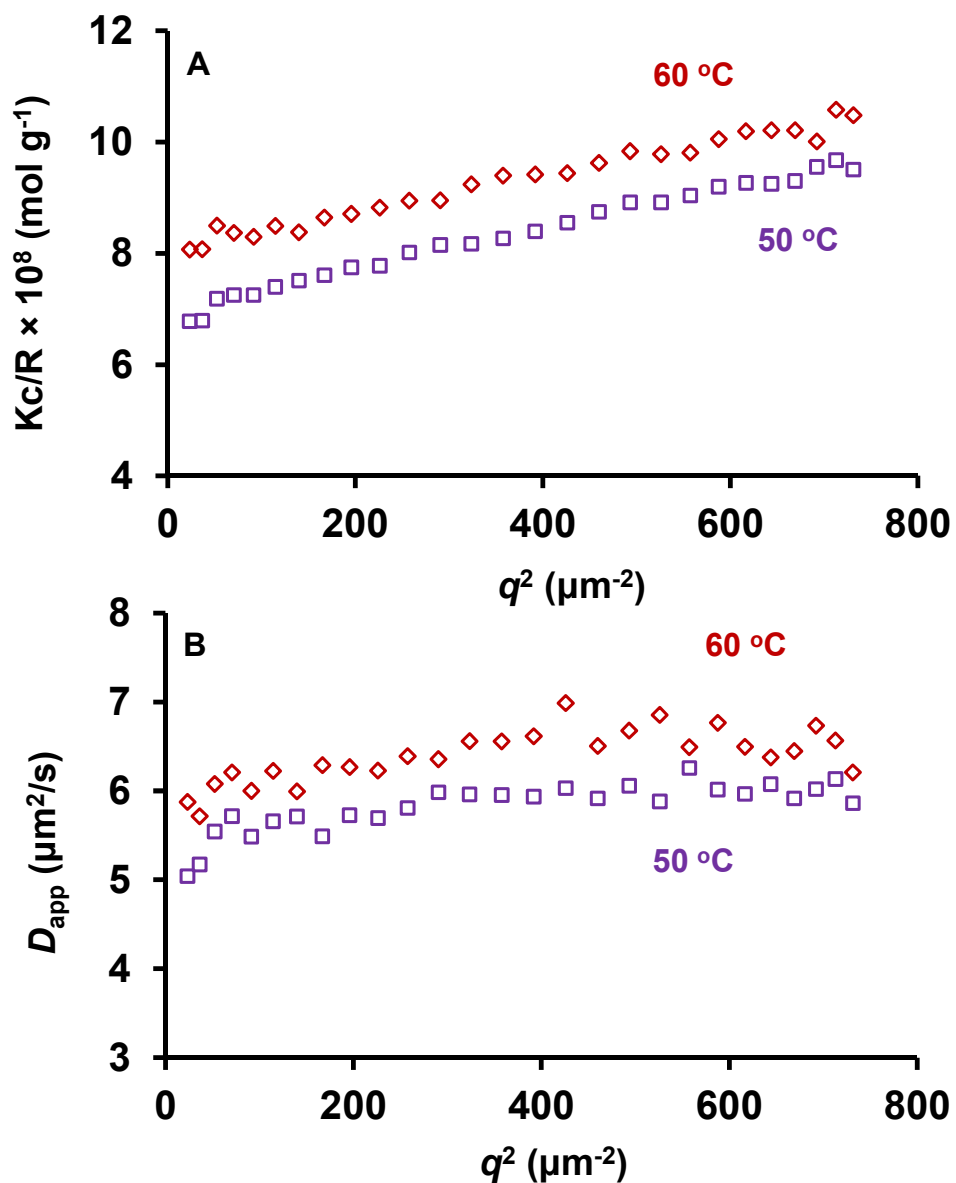


**Figure S3:** A) Plot of  $Kc/R$  versus  $q^2$  for a  $\text{PFS}_{53}\text{-}b\text{-PI}_{637}$  seed solution after they were annealed for 30 min at 50 °C (purple open squares), and at 60 °C (brown diamonds). B) Plot of the diffusion coefficient,  $D_{\text{app}} = \Gamma/q^2$ , versus  $q^2$ , where  $\Gamma$  is the decay rate for the same solutions as in A). The concentration of the solution for the self-seeding experiments was  $c = 6.0 \text{ mg mL}^{-1}$  and the samples were diluted to a concentration  $c = 0.01 \text{ mg mL}^{-1}$  before performing the SLS and DLS experiments.

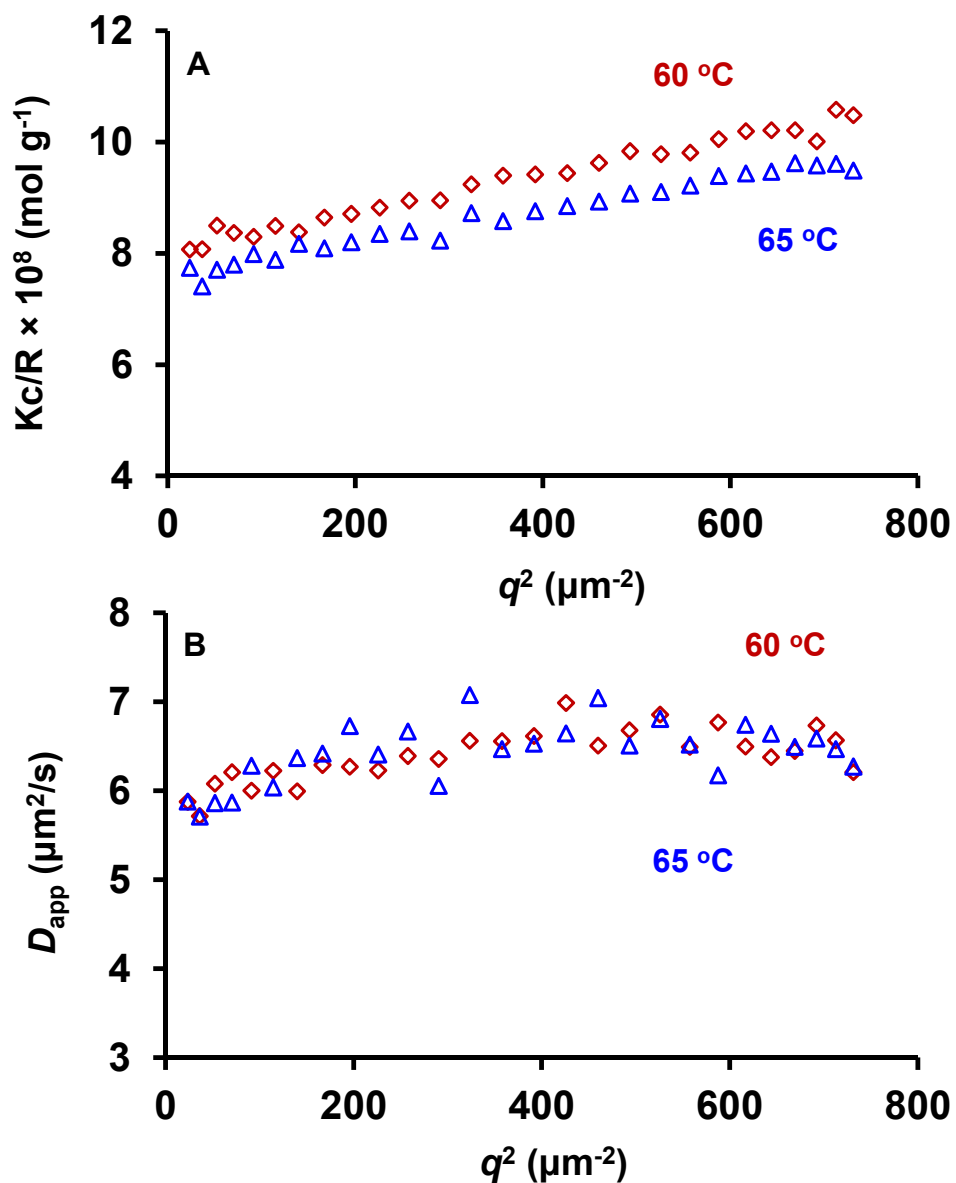


**Figure S4:** A) Plot of  $Kc/R$  versus  $q^2$  for a  $\text{PFS}_{53}\text{-}b\text{-PI}_{637}$  seed solution after they were annealed for 30 min at 60 °C (brown diamonds), and at 65 °C (blue triangles). B) Plot of the diffusion coefficient,  $D_{\text{app}} = \Gamma/q^2$ , versus  $q^2$ , where  $\Gamma$  is the decay rate for the same solutions as in A). The concentration of the solution for the self-seeding experiments was  $c = 6.0 \text{ mg mL}^{-1}$  and the samples were diluted to a concentration  $c = 0.01 \text{ mg mL}^{-1}$  before performing the SLS and DLS experiments.

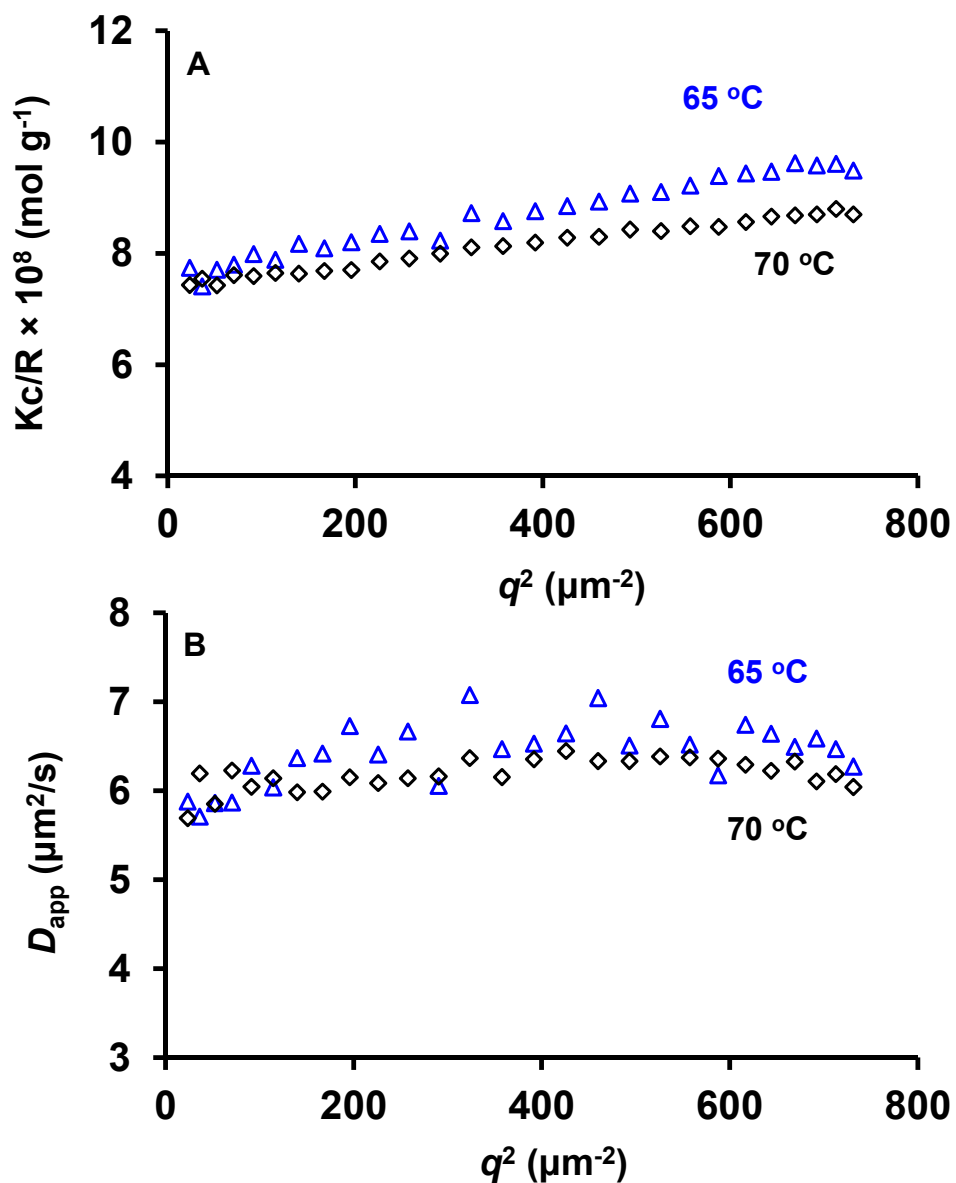


**Figure S5:** A) Plot of  $Kc/R$  versus  $q^2$  for a  $\text{PFS}_{53}\text{-}b\text{-PI}_{637}$  seed solution after they were annealed for 30 min at 65 °C (blue triangles), and at 70 °C (black diamonds). B) Plot of the diffusion coefficient,  $D_{\text{app}} = \Gamma/q^2$ , versus  $q^2$ , where  $\Gamma$  is the decay rate for the same solutions as in A). The concentration of the solution for the self-seeding experiments was  $c = 6.0 \text{ mg mL}^{-1}$  and the samples were diluted to a concentration  $c = 0.01 \text{ mg mL}^{-1}$  before performing the SLS and DLS experiments.



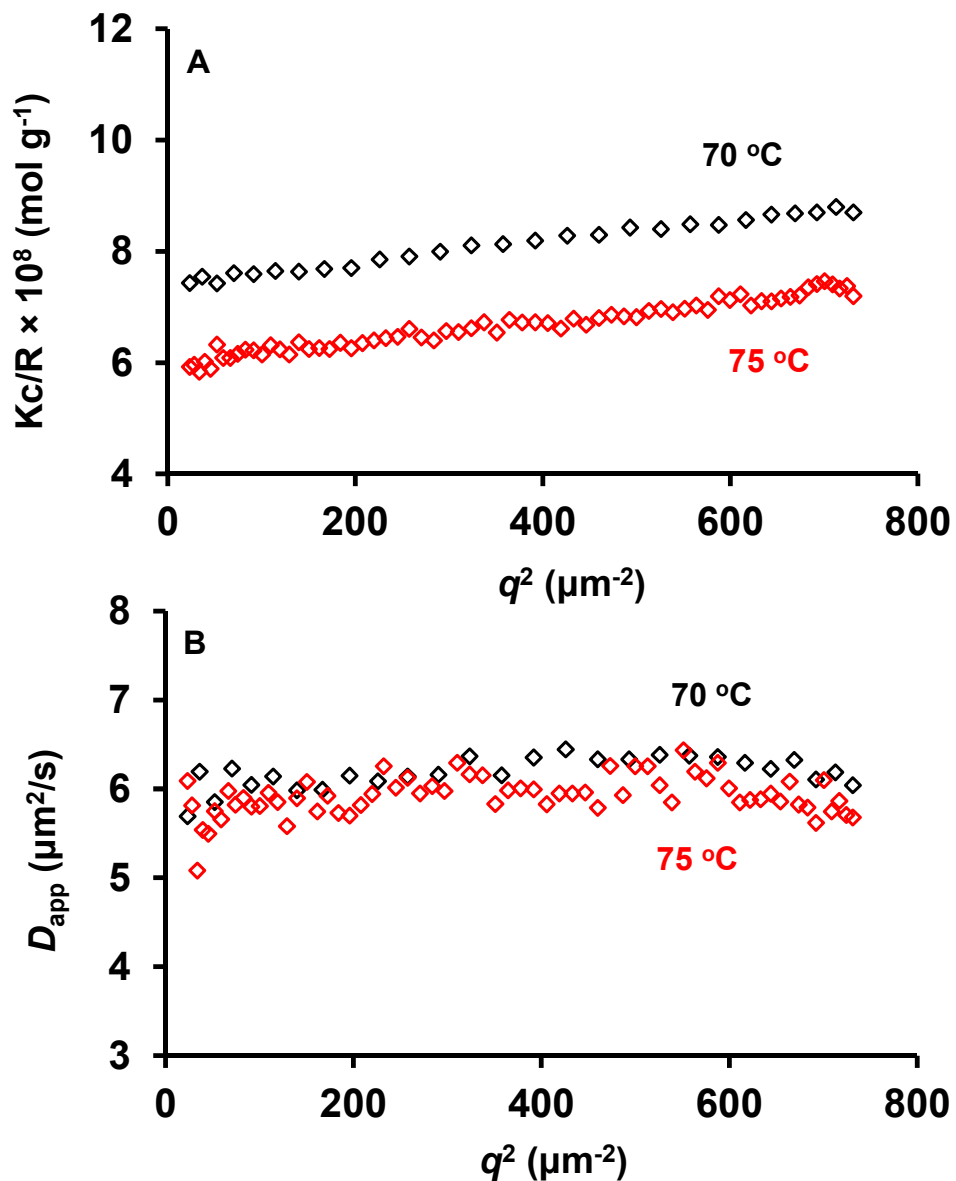


**Figure S6:** A) Plot of  $Kc/R$  versus  $q^2$  for a  $\text{PFS}_{53}\text{-}b\text{-PI}_{637}$  seed solution after they were annealed for 30 min at 70 °C (black diamonds), and at 75 °C (red diamonds). B) Plot of the diffusion coefficient,  $D_{\text{app}} = \Gamma/q^2$ , versus  $q^2$ , where  $\Gamma$  is the decay rate for the same solutions as in A). The concentration of the solution for the self-seeding experiments was  $c = 6.0 \text{ mg mL}^{-1}$  and the samples were diluted to a concentration  $c = 0.01 \text{ mg mL}^{-1}$  before performing the SLS and DLS experiments.

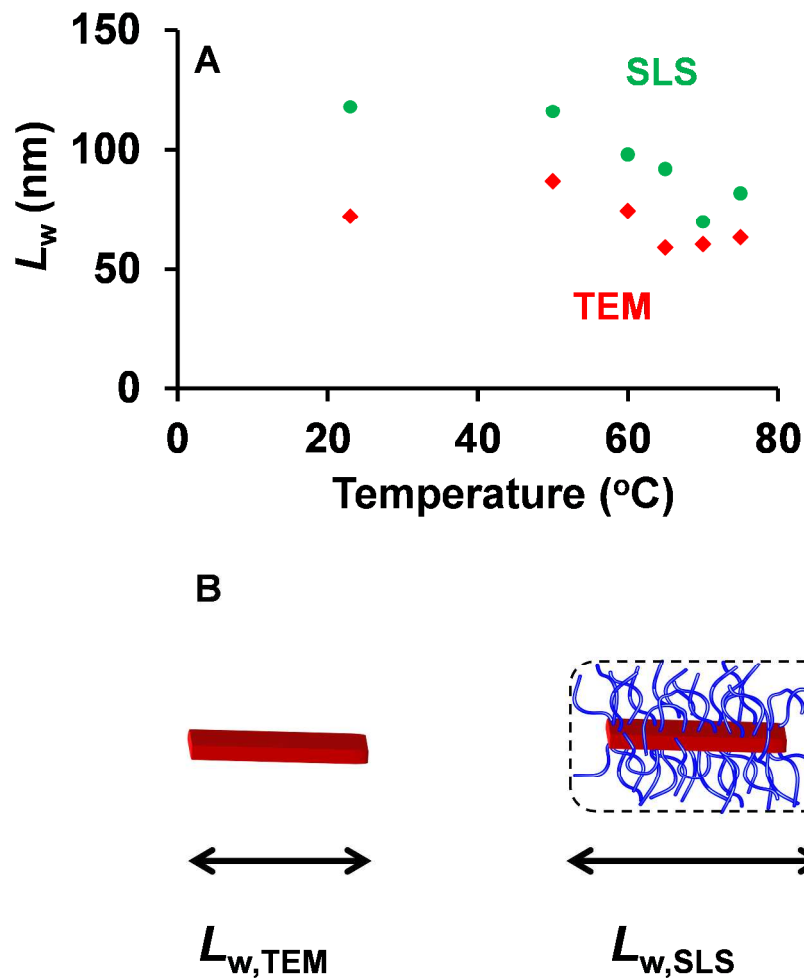


**Figure S7:** A) Plot of the weight average length evaluated from TEM image analysis,  $L_{w,TEM}$ , and from the SLS data fitted with equation 2, main text,  $L_{w,SLS}$ . B) Schematic representation of seed micelle fragments of PFS<sub>53</sub>-b-PI<sub>637</sub> as observed by TEM and by SLS. We hypothesize that in solution, the presence of corona chains protruding from the seed core leads to larger values of their weight average length than those evaluated by TEM image analysis, where the corona chains are hardly visible. For much longer micelles, the difference between these two measures would not be significant.

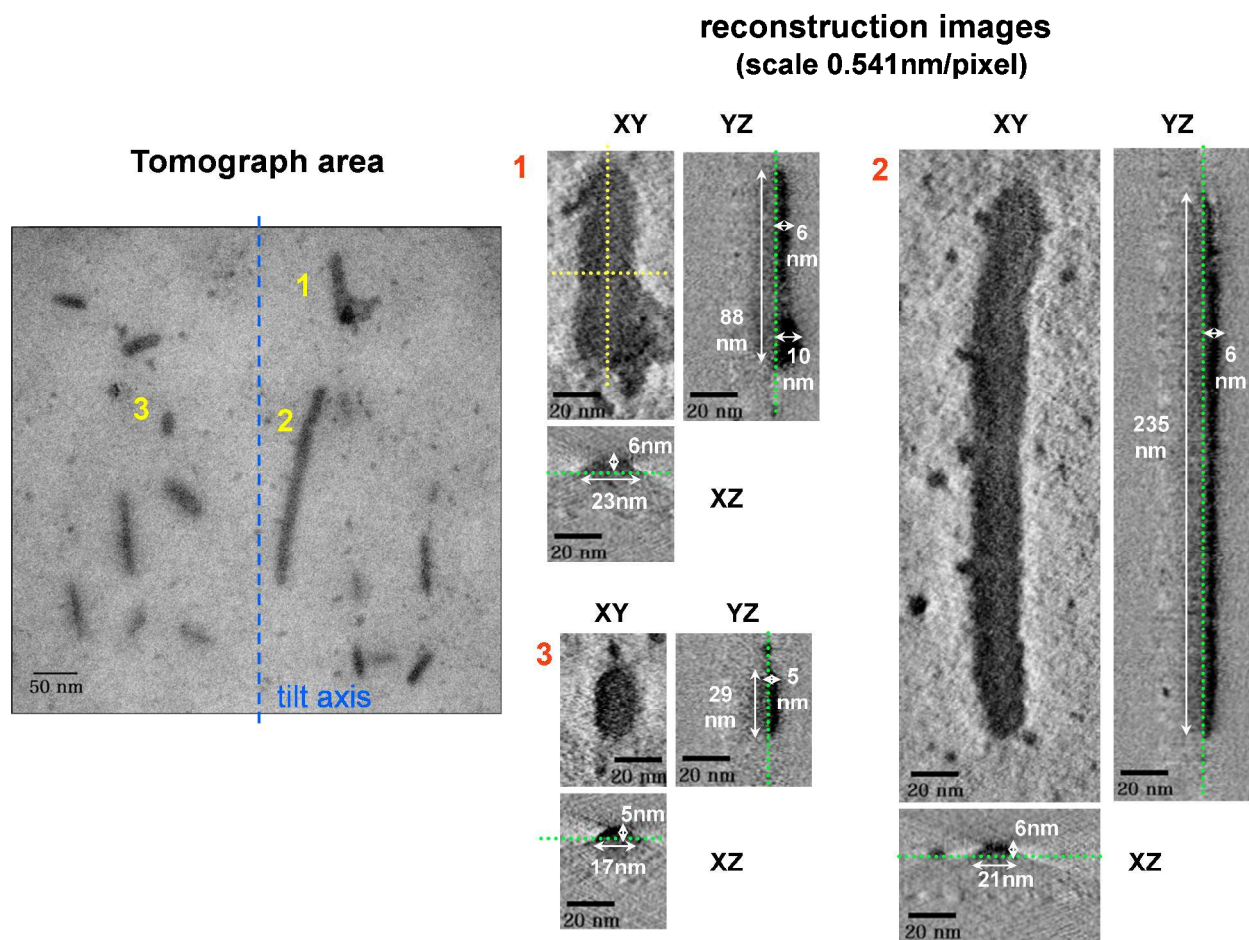


**Figure S8:** Electron tomography images of PFS<sub>53</sub>-*b*-PI<sub>637</sub> seeds annealed for 30 minutes at 50 °C For each micelle studied three orthogonal cross-sectional views are shown from the XY, YZ and XZ planes.

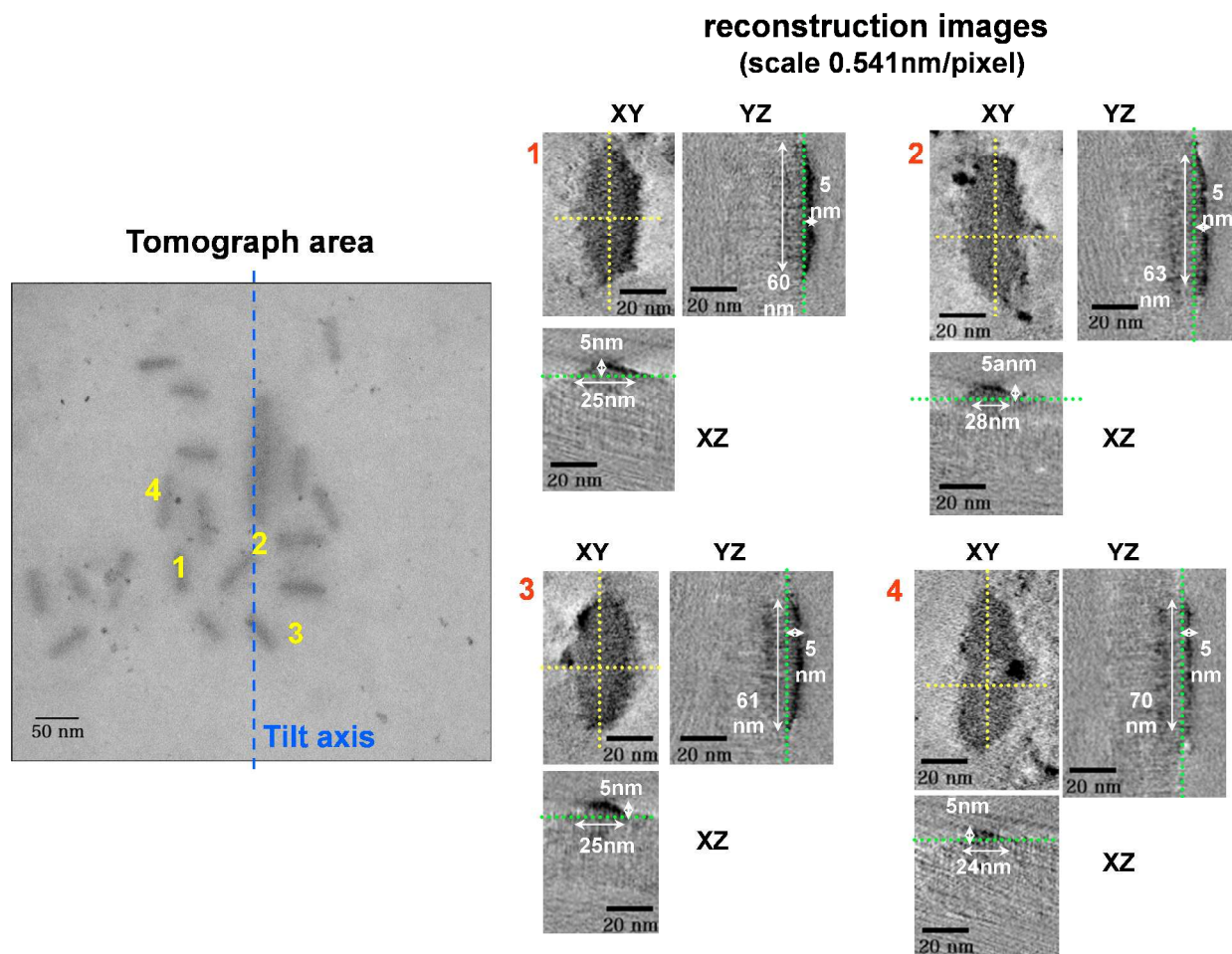


**Figure S9:** Electron tomography images of  $\text{PFS}_{53}\text{-}b\text{-PI}_{637}$  seeds annealed for 30 minutes at 75 °C For each micelle studied three orthogonal cross-sectional views are shown from the XY, YZ and XZ planes.